Alternative robotic control methods that account for system compliance decrease the errors in ligament tensions computed using the superposition method

Lesley R. Arant, first author[1]
Department of Biomedical Engineering, University of Wisconsin – Madison
1111 Highland Avenue Room 5059, Madison, WI 53706
larant@wisc.edu

Joshua D. Roth, second author
Department of Orthopedics and Rehabilitation and Department of Mechanical Engineering, University of Wisconsin – Madison
1111 Highland Avenue Room 5059, Madison, WI 53706
roth@ortho.wisc.edu

Abstract

Superposition testing is a method to quantify *in situ* ligament tension by measuring the change in joint loads before and after ligament sectioning. Despite its widespread use, the traditional robot control method used in superposition testing may introduce errors because it does not account for system compliance when prescribing joint kinematics. Therefore, our objective was to quantify the errors in superposition-computed tensions using the robot control method, and to validate a novel motion capture control method that accounts for system compliance by measuring joint kinematics using optical motion capture sensors fixed to the bones. Using our robotic testing system, we performed superposition testing to quantify lateral collateral ligament tension in five cadaveric knees during prescribed varus and external rotation loading trajectories using both robot control and motion capture control. We computed the errors between superposition-computed tensions and gold-standard ligament tensions measured by an in-series load cell. Compared to robot control, we found that motion

[1] Corresponding author: Lesley Arant, larant@wisc.edu

capture control significantly decreased the errors in superposition-computed tensions in the lateral collateral ligament during both varus (from -92 ± 30 N to -27 ± 21 N) and external rotation (from -27 ± 19 N to -10 ± 9 N) loading by decreasing errors in joint kinematics and bone positions. Thus, we recommend implementing a control method that accounts for system compliance to achieve low errors in superposition-computed tensions for a particular robotic testing system and ligament type. With proper reporting of errors, superposition testing will continue to be a valuable experimental method to quantify *in situ* ligament tensions.

1 Introduction

Superposition testing, also known as sequential sectioning, is an established method used since the mid 1990's to quantify *in situ* ligament tension using a robotic testing system equipped with a six-degree-of-freedom load cell [1]. In this method, first, the robot prescribes kinetics to an intact joint to tension a ligament of interest while joint kinematics are recorded. Then, the recorded kinematics are prescribed to the joint before and after sectioning that ligament. Ligament tension is then computed as the vector difference in joint loads between the ligament-intact and ligament-deficient joint states [1]. Superposition testing has been widely used in a variety of joints to quantify native ligament tensions [2-4], and to determine the effects of injury [5, 6], growth [7], and surgical interventions [8, 9] on ligament mechanics.

Despite its long-standing and widespread use, the superposition method to measure ligament tensions has not been validated in cadaveric joints, and the traditional control method used in superposition testing may introduce errors depending on the testing system. In the traditional control method, known herein as robot control, all components of the testing system except the joint are assumed to be infinitely rigid. Thus, the position of the robot-mounted bone (e.g., femur) is determined by applying rigid transformations from (1) the robot base to the robot end effector, and (2) the robot end effector to the position of the robot-mounted bone at the joint [10]. The position of the other bone in the joint (e.g., tibia), which is usually mounted to a stiff pedestal base, is assumed to be fixed. However, because this control method does not account for compliance in the system including the robot, fixtures, and bones, it may result in errors

in joint kinematics between the intact and ligament-deficient joint states, and thus errors in superposition-computed tensions [11, 12].

An alternative control method, referred to herein as motion capture control, may decrease the errors in joint kinematics and superposition-computed tensions caused by system compliance. In motion capture control, joint kinematics are measured by tracking optical motion capture sensor(s) rigidly attached to the bones [12, 13]. If these sensor(s) are placed close to the joint and have high signal-to-noise ratios, then they capture the true joint kinematics, regardless of system compliance. Therefore, motion capture control may result in more accurate tensions when used in the superposition method compared to robot control. While motion capture control has demonstrated low errors in kinematics and superposition-computed tensions in a surrogate knee joint [12, 13], it has not been directly validated in human cadaveric joints. Additionally, it is unknown whether motion capture control needs to be implemented for both the robot-mounted bone and the fixed bone, or only the robot-mounted bone, to effectively account for system compliance and reduce the errors in superposition-computed tensions.

Therefore, the objectives of this study were to: (1) Quantify the errors in superposition-computed tensions using the traditional robot control method, (2) Validate motion capture control as an alternative control method to decrease the errors in superposition-computed tensions, and (3) Quantify and compare the errors in joint kinematics and bone positions for each control method and determine their effects on the errors in superposition-computed tensions. We hypothesized that the robot control method would result in higher errors in superposition-computed tensions and joint kinematics compared to motion capture control because it does not account for system

compliance. We used the lateral collateral ligament (LCL) of the knee as a representative ligament in this study.

2 Methods

2.1 Specimen Preparation

We procured five, fresh-frozen, human cadaver knees (2M/3F, 65.6 ± 4.9 years, 165.6 ± 8.5 cm, 67.6 ± 19.8 kg) for robotic testing. We set this sample size based on an *a priori* power analysis to detect differences in tension errors between the robot and full motion capture control methods of 1.9 ± 0.3 N. This mean difference is 10% of the mean difference in tension errors between the robot and full motion capture control methods from three repeated trials in a surrogate knee, and thus is a conservative estimate of the expected difference in errors [12, 13]. We determined that at least three specimens were required to detect the specified errors with a significance level (α) = 0.05 and a power (1-β) = 0.9.

We prepared each knee for testing using the following steps. First, we fixed the fibula to the tibia using a transverse screw inserted just distal to the fibular head to maintain the native position of the fibula relative to the tibia. We then transected the fibula 25 mm distal to this screw. We potted the femur and tibia in aluminum tubes (Bondo, 3M) to enable rigid mounting of each bone to our robotic testing system. We use precision clamps to connect these tubes to our robot.

To quantify the errors in superposition-computed tensions, we developed a novel method to measure gold-standard tension in the LCL (**Fig. 1**). We chose the LCL because it is a superficial ligament with an insertion that can be isolated and directly connected to a load cell for gold-standard tension measurements. First, we centered an aluminum core

with a threaded hole in a 1-inch diameter plastic sleeve using a temporary holder. Then, we potted the inferior end of the proximal fibula in the plastic sleeve (Bondo, 3M) to create a cylinder that encompassed the fibula proximally and the aluminum core with the threaded hole distally. Next, we resected the articular surfaces of the proximal tibiofibular joint to prevent any contact between the fibula and the tibia. We also resected all soft tissues attached to the fibular head except for the LCL. Then, we zeroed a six-axis load cell (ATI Delta IP65, SI-660-60 calibration) and attached the aluminum core of the potted fibula to the load cell. This load cell will be referred to herein as the LCL load cell. See **Supplement S.1, Table S1** for the sensing ranges and resolutions of the LCL load cell. Finally, we removed the transverse screw fixing the fibula to the tibia to ensure that all the tension in the LCL was transmitted to the LCL load cell. We used a six-axis load cell because it enabled rigid fixation of the fibula in its anatomic location while capturing off-axis loads. A similar setup has been used previously in the cruciate ligaments [14, 15]. We computed gold-standard LCL tension as the resultant force measured by the LCL load cell. We confirmed that the stiffness of the fixture attaching the potted fibula to the LCL load cell was high so it did not introduce errors in gold-standard LCL tension (**Supplement S.2, Figure S1**).

2.2 Motion Capture System Setup

We positioned four optical motion capture cameras (Optitrack Prime 13×; NaturalPoint Inc.) such that the capture volume was limited to the volume the specimen would be moving within, during robotic testing (**Fig. 2a**). We used screws to rigidly attach custom motion capture sensors to the shafts of the tibia and the femur as close to the joint line without disrupting any soft tissue attachments (**Fig. 1**). The rigid body positions

(i.e., x, y, z, roll, pitch, yaw) of these sensors were tracked by the optical motion capture cameras and software. We designed the motion capture sensors to include four 0.25-inch diameter markers arranged such that: (1) the markers were not planar, and (2) each marker was visible by each camera in every joint pose. We chose this motion capture system setup because in preliminary testing, we identified maximum tracking precision with this combination of camera positioning and sensor design. We measured the root mean square error of marker tracking using this optical motion capture system setup to be 59 μm (**Supplement S.3**).

2.3 Robotic Testing

We mounted each knee to our robotic testing system using the following steps. First, we fixed the tibia of each knee to a rigid pedestal base in series with a six-axis load cell (ATI Omega160 IP65, SI-1000-120 calibration) used to measure and control joint kinetics (**Fig. 1**). This load cell will be referred to herein as the control load cell. See **Supplement S.1, Table S1** for the sensing ranges and resolutions of the control load cell. We also mounted the LCL load cell to the pedestal base (**Fig. 1**), and we zeroed the weight of the LCL load cell from the control load cell measurements. We mounted the femur of each knee to our six-degree-of-freedom robotic testing system (KR300-R2700; KUKA Robotics, reported pose repeatability = 50 μm) controlled with simVITRO® software [10] (**Fig. 2a**). We measured the maximum stiffness of our robot to be 1338 N/mm in the +X direction and the minimum stiffness to be 551 N/mm in the -Y direction, which is similar to other serial Kuka robots of comparable size (**Supplement S.4, Table S2**).

After mounting the specimen to the robot, we digitized anatomical landmarks of the knee using our optical motion capture system to establish an initial joint coordinate

system [16]. We then defined a functional coordinate system that minimized kinematic cross-talk [17] between the primary degrees-of-freedom (i.e., flexion-extension and internal-external rotation) and secondary degrees-of-freedom (i.e., varus-valgus rotation, and anterior-posterior, medial-lateral, and compression-distraction translation) during prescribed passive flexion-extension and internal-external rotation trajectories [18]. We defined full extension as the flexion-extension angle of the knee under an extension moment of 2.5 Nm [14].

We then prescribed kinetic-control trajectories to tension the LCL. These included: (1) varus ramp loading and unloading at a rate of 0.6 Nm/s to a maximum torque of 15 Nm, and (2) external rotation ramp loading and unloading at a rate of 0.2 Nm/s to a maximum torque of 5 Nm. During both ramp trajectories, we prescribed 50 N of compression and minimized other off-axis loads. We prescribed both trajectories at 0°, 30°, 60°, and 90° knee flexion. The order of the flexion angles as well as the order of the primary loading direction (varus or external rotation) within each flexion angle were randomized for each specimen. To precondition the soft tissues in the knee, we prescribed 10 cycles of each of these trajectories and confirmed that the peak LCL tension, as measured by the LCL load cell, plateaued by the tenth cycle (**Supplement S.5, Figure S4**).

After preconditioning, we prescribed 1 cycle of the same varus and external rotation loading trajectories at each flexion angle. We recorded the joint kinematics using three different methods to track the position of the femur and tibia (**Table 1**). First, we measured joint kinematics using the traditional robotic testing method, wherein the femur was tracked using the position of the robot end effector, and the tibia was assumed fixed.

These kinematics are referred to herein as robot kinematics. Second, both the femur and tibia were tracked using the positions of the motion capture sensors, referred to herein as full motion capture kinematics. Third, the femur was tracked using the position of the motion capture sensor, while the tibia was assumed fixed, referred to herein as partial motion capture kinematics.

Next, we performed superposition testing to determine the LCL tension using three different control methods implemented using eXactoPOSE® (**Fig. 2b**). eXactoPOSE® is a novel control algorithm that uses sensor fusion to measure and control joint kinematics [12, 13]. Using eXactoPOSE®, we prescribed kinematics using robot control, full motion capture control, and partial motion capture control, during which the control kinematics were the corresponding kinematics measured during the kinetic-control trajectories (e.g., full motion capture control prescribed and controlled full motion capture kinematics). We prescribed each trajectory (i.e., varus and external rotation at each flexion angle) for each control method in the same randomized order as the kinetic-control loading, and we randomized the order of the control methods for each specimen. For each test, we recorded the joint kinetics, full motion capture kinematics, positions of the femur and tibia motion capture sensors, and the gold-standard LCL tensions as measured by the LCL load cell. We low-pass filtered the joint kinetics and LCL tensions using a 0.2 Hz cut-off frequency.

We then disconnected the potted fibula from the LCL load cell and prescribed the same kinematics for each of the three control methods to the LCL-deficient joint (**Fig. 2b**). We followed the same randomization order from the intact testing and recorded the joint kinetics, full motion capture kinematics, and positions of the femur and tibia motion

capture sensors. We computed the tension in the LCL (i.e., superposition-computed tension) for each test as the vector difference in the low-pass filtered joint forces between the intact and LCL-deficient states (**Fig. 2b**) [1]. We also computed the errors in kinematic tracking of the desired trajectory to characterize the performance of the kinematic controller (**Supplement S.6, Table S3**).

2.4 Error Analysis

To address the first two objectives, we performed an error analysis on the superposition-computed tensions to characterize and compare the performance of each control method. First, we computed the errors in superposition-computed tensions as the difference between the superposition-computed and LCL load cell-measured tensions in the LCL for each trial. Then, we pooled these errors across specimens and flexion angles and computed the bias (mean) and precision (standard deviation) errors for each control method and primary loading direction (varus or external) following ASTM E177-20 [19]. We also computed the bias and precision errors for the errors at the peak LCL tension, as measured by the LCL load cell, for each trial. Finally, we fit linear mixed models to identify significant differences in the errors in superposition-computed tension at peak tension between the three control methods (level of significance, α, = 0.05). We only performed statistical tests on the peak tensions because the full dataset contained over 600,000 points from each group being compared, so even small differences were statistically significant. In the linear mixed models, the control method was modeled as a fixed effect, and both specimen and flexion angle were modeled as random effects, with flexion angle nested in specimen. We performed separate linear mixed models for the

varus and external rotation loading data. We extracted the p-values from post-hoc Tukey tests for pairwise comparisons of the three control methods.

To address the third objective, we performed error analyses on the joint kinematics and bone positions. First, we computed the errors in motion capture kinematics as the magnitude of the vector differences in motion capture translations between the intact and LCL-deficient joint states. Second, we computed the errors in the positions of the femur and tibia motion capture sensors as the magnitude of the vector differences in the x, y, and z positions of the motion capture sensors between the intact and LCL-deficient joint states. We computed the bias and precision errors as we did for the superposition-computed tension errors. Finally, we fit linear mixed models to identify significant differences in the errors in kinematics, femur sensor positions, and tibia sensor positions at peak tension between the three control methods (level of significance, α, = 0.05). In the linear mixed models, the control method was modeled as a fixed effect, and both specimen and flexion angle were modeled as random effects, with flexion angle nested in specimen. We performed separate linear mixed models for the varus and external rotation loading data. We extracted the p-values from post-hoc Tukey tests for pairwise comparisons of the three control methods.

Finally, to determine the relationship between kinematics errors and superposition-computed tension errors, we performed simple linear regressions between the errors in motion capture kinematics (independent variable) and the errors in superposition-computed tensions (dependent variable) at peak tension for each control method and primary loading direction. We extracted the p-values and R^2 to evaluate the significance and strength, respectively, of each relationship.

3 Results

Using the traditional robot control method in superposition testing, the superposition-computed LCL tensions underestimated the true LCL tensions for both varus and external rotation loading trajectories (**Fig. 3**). The average errors reached -92 ± 30 N (-64 ± 11% error) and -27 ± 19 N (-33 ± 70% error) at peak tension for varus and external rotation loading, respectively. In contrast, when we implemented partial motion capture and full motion capture control using eXactoPOSE®, the errors in superposition-computed tensions significantly decreased (**Fig. 3**). The average errors at peak tension were smallest for partial motion capture control, where they decreased by factors of 5.4 and 4.5 for varus and external rotation loading, respectively, compared to traditional robot control. Still, on average, superposition testing using partial and full motion capture control underestimated LCL tension.

The errors in the motion capture kinematics between the intact and LCL-deficient joints at peak LCL tension were significantly higher for the robot control method compared to those for the partial and full motion capture control methods (**Fig. 4**). Even for the robot control method, the errors (150 ± 67 μm and 111 ± 98 μm at peak tension for varus and external rotation loading, respectively) were relatively small compared to the magnitude of the kinematic excursions in the intact knee, which we determined to be 1947 ± 824 μm and 1336 ± 729 μm at peak tension for varus and external rotation loading, respectively. The average errors at peak tension were smallest for the full motion capture control method, where they decreased by factors of 4.3 and 3.9 for varus and external rotation loading, respectively, compared to the robot control method.

The errors in the position of the femur sensor between the intact and LCL-deficient joints at peak LCL tension were significantly higher for robot control compared to those for partial motion capture control (**Fig. 5**). The errors were also significantly higher for robot control compared to those for full motion capture control during varus loading only. We found the smallest errors for the partial motion capture control method. Similarly, during varus loading trajectories, the errors in the position of the tibia sensor between the intact and LCL-deficient joints at peak LCL tension were significantly higher for robot control compared to those for partial motion capture control (**Fig. 6**). We did not find any significant differences in the tibia sensor errors between control methods during external loading.

For the robot control method, we found significant ($p<0.001$), positive relationships between the magnitude of the errors in motion capture translations and the magnitude of the errors in superposition-computed LCL tensions at peak tension for both varus and external rotation loading (**Fig. 7**). For the partial and full motion capture control methods, the errors in both kinematics and tension were smaller, and we did not find a significant relationship between the errors ($p>0.001$).

4 Discussion

Superposition testing to determine ligament tensions *in situ* has not been directly validated, and analytical evaluations of spring models suggest that the traditional robot control method may introduce errors in superposition-computed tensions and joint kinematics [13, 20]. Therefore, the objectives of this study were to: (1) Quantify the errors in superposition-computed tensions using the traditional robot control method, (2) Validate motion capture control as an alternative control method to decrease the errors

in superposition-computed tensions, and (3) Quantify and compare the errors in joint kinematics and bone positions for each control method and determine their effects on the errors in superposition-computed tensions. Our first key finding was that superposition-computed LCL tensions measured using the traditional robot control method underestimated the true LCL tensions with average errors at peak tension of -64% and -33% for varus and external rotation loading, respectively. Our second key finding was that implementing motion capture control significantly decreased the errors at peak tension by factors of up to 5.4. Our third key finding was that errors in joint kinematics and bone positions were highest for the traditional robot control method, and there were significant, positive relationships between the errors in joint kinematics and the errors in superposition-computed tensions. Therefore, our results support our hypothesis that motion capture control results in lower errors in superposition-computed LCL tensions and joint kinematics compared to the traditional robot control method for our particular robotic testing system and motion capture system.

The first key finding was that the superposition method using the traditional robot control method underestimated the true LCL tensions in cadaver knees (**Fig. 3**). This is consistent with prior findings in a surrogate knee [12, 13] and an analytical evaluation of the effects of system compliance on superposition-computed tension errors using a spring model [20, 21]. The average errors in superposition-computed LCL tensions at peak varus loading were higher in the cadaver knees than those in a surrogate knee (-64% vs. -23%). This is likely because cadaver knees are stiffer than the surrogate knee, and errors in superposition-computed tension are expected to increase with increased specimen stiffness [20, 21]. The implications of these systematic errors in superposition-computed

tensions using the traditional robot control method can be large, particularly because small changes in ligament tension are known to result in large changes in joint kinematics [22]. While relative trends observed from superposition testing using the robot control method are likely valid, absolute ligament tensions obtained from joints and robotic testing systems of similar stiffnesses as those in this study should be interpreted with caution, especially when used to inform clinical decisions. Additionally, without an understanding of the errors for a particular robotic testing system and control method, the use of superposition-computed tensions as gold-standard ligament tensions for applications including sensor validation and musculoskeletal models should be avoided.

The second key finding that implementing motion capture control using eXactoPOSE® significantly decreased the errors in superposition-computed LCL tensions indicates that motion capture control is a promising alternative to traditional robot control (**Fig. 3**). The average errors at peak varus loading decreased from -64% for the traditional robot control method to -14% for the partial motion capture control method and -21% for the full motion capture control method. These reductions in errors are consistent with pilot validation results in a surrogate knee [12, 13]. While the errors were, on average, smaller for partial compared to full motion capture control, the difference did not reach statistical significance. Thus, either motion capture control method may be a favorable alternative to robot control.

Our third key finding was that errors in joint kinematics and bone positions were highest for the traditional robot control method (**Figs. 4-6**), and there was a significant relationship between the errors in joint kinematics and the errors in superposition-computed tensions (**Fig. 7**). Gillespie et al. describes the mechanism relating the errors

in kinematics to the errors in superposition-computed tensions that we measured in this study [13, 20]. To summarize, after a ligament is removed, the loads applied to the robot decrease. Because the robot is not infinitely rigid, the robot deflects, as does the bone mounted to the robot. This is consistent with our results, which show that the joint and the femur are not in the same position before and after ligament resection (**Figs. 4 and 5**). When the femur deflects, the tension in the secondary restraints increases and the contact forces decrease, resulting in an increase in the loads measured by the control load cell (**Fig. 8**). Therefore, the difference in loads between the intact and ligament-deficient joints, and thus the superposition-computed tensions, are underestimated. Our results also indicate that motion capture control can correct the errors in kinematics between the intact and ligament-deficient conditions (**Fig. 4**). Motion capture sensors directly measure the positions of the bones, and thus effectively correct for the deflection of the robot-mounted bone after removing the ligament [12]. By controlling the robot to achieve repeatable kinematics regardless of system compliance, the intact and ligament-deficient kinematics better match, and errors in superposition-computed LCL tension are reduced (**Fig. 7**).

Given this mechanism, we expect the errors in superposition-computed tensions using robot control to decrease with increased robot stiffness and decreased specimen stiffness [20]. In a robot with greater stiffness, the robot will deflect less under the difference in loads between the intact and ligament-deficient conditions. Thus, to minimize the errors in superposition-computed tensions for any specimen, robot stiffness should be maximized. The importance of high robot stiffness to achieve repeatable joint motion has been recognized in the robotic biomechanics testing community [11, 23-26], but our

results are the first we are aware of to demonstrate the implications of robot compliance on superposition testing with an industrial robot commonly used in joint biomechanics testing. Other robots, such as parallel robots, may be stiffer, and thus achieve smaller errors in superposition-computed tensions [20, 21]. Additionally, we expect errors in superposition-computed tension to be smaller in ligaments that are aligned with less-stiff degrees-of-freedom, such as the anterior cruciate ligament. In a less stiff degree-of-freedom, the same robot deflection will result in a smaller change in joint loads. Conversely, stiffer specimens, such as those with metallic implants, may have higher errors in superposition-computed ligament tensions. However, additional studies are required to confirm these expected trends, and they highlight the need for each group to validate their robotic testing system within their unique context(s) of use.

The limited precision of our motion capture system may explain: (1) the remaining errors in superposition-computed tension using either motion capture control method, and (2) the slightly larger errors in superposition-computed tensions for full motion capture control compared to partial motion capture control. First, for both motion capture control methods, the remaining errors in kinematics (**Fig. 4**) and bone positions (**Figs. 5 and 6**) are on the order of the root mean square error of marker tracking using our motion capture system (**Supplement S.3**). Therefore, small errors in the measured bone positions using motion capture likely limit the minimum errors in superposition-computed tensions that can be achieved using motion capture control. Second, the difference in the errors in kinematics and bone positions between partial and full motion capture control are often below the RMSE of our motion capture system. This makes it difficult to identify the source of the slightly larger errors in superposition-computed tensions for the full compared to

the partial motion capture control methods (**Fig. 3**). One possible explanation is that, in the full motion capture control method, the noise from the additional motion capture sensor on the tibia outweighs the advantage of accounting for compliance in the tibia and pedestal base. Based on our data, the tibia can be assumed to be sufficiently fixed (**Fig. 6**). However, this assumption may differ according to the fixation method of the tibia to the pedestal base as well as the stiffness of the pedestal base. For implementing either motion capture control method, we recommend identifying an optical motion capture system and camera configuration that maximize the tracking precision in order to decrease the errors in kinematics, and thus, decrease the errors in superposition-computed tensions.

One limitation of eXactoPOSE is that it works under the assumption that if the motion capture sensors fixed to the bones are in the same position in the ligament-intact and ligament-deficient knee states, the ligament attachment locations will be in the same positions. That is, eXactoPOSE controls joint kinematics, not ligament kinematics. However, given that motion capture sensors were attached close to the joint, there is not substantial compliance between the motion capture sensor attachment locations and the ligament attachment locations. Thus, using eXactoPOSE to accurately recreate joint kinematics effectively recreates ligament kinematics, leading to more accurate superposition-computed tensions than when using the robot control method.

There are two limitations of this study that should be considered when interpreting the findings. The first limitation is that we quantified the errors in superposition-computed tensions for one ligament type, one cadaveric joint type, one robotic testing system, and one motion capture system. As described previously, we expect errors to vary with

different systems and/or context(s) of use. However, given our cadaveric results, along with supporting results from a surrogate knee [12] and analytical spring models [20, 21], we expect other systems to also demonstrate an underestimation in superposition-computed ligament tension using the traditional robot control method, and a reduction in errors when implementing a control method that accounts for compliance (e.g., motion capture control). The second limitation of this study is the limited sample size. While we successfully procured specimens of different sexes, heights, and weights, the five samples do not represent the wide range of knee health and disease states of the cadaveric joints in which superposition testing is used. While we do expect the magnitude of the errors in superposition-computed tension using robot control to vary in different specimens according to their joint stiffness, we do not expect the trends to vary. Therefore, for the purposes of demonstrating an underestimation of superposition-computed tensions using robot control, and the promise of an alternative control method using motion capture control, this sample size was sufficient.

5 Summary

This study is the first, to our knowledge, to directly quantify the errors in *in situ* ligament tensions computed using superposition testing. We found that the traditional robot control method used in superposition testing can underestimate LCL tensions by as much as 64%. Using the traditional robot control method, errors in joint kinematics between the intact and ligament-deficient states caused by robot compliance violate a fundamental assumption in superposition testing and lead to errors in superposition-computed tensions. Motion capture control implemented using eXactoPOSE® is a promising alternative control method to significantly decrease the errors in superposition-

computed tensions. Motion capture control was able to achieve smaller errors in superposition-computed LCL tensions by achieving more similar kinematics between the intact and ligament-deficient states.

Superposition testing has been and will continue to be a valuable experimental approach to quantify ligament tensions to understand the effects of disease, injury, and surgical interventions. For robot and motion capture control methods, it is necessary to report the errors in superposition-computed tensions to properly interpret the reported ligament tensions, especially because errors will vary with different robotic testing and motion capture systems. Based on our results, we recommend adopting a control method for superposition testing that accounts for system compliance (e.g., motion capture control) over the traditional robot control method to significantly reduce the errors in superposition-computed ligament tensions in specimens and robotic testing systems of similar stiffness to those used in this study.

Acknowledgment

We acknowledge the technical support of the simVITRO® team to implement eXactoPOSE®, and the statistical support from Sam Mosiman to implement the linear mixed models.

Funding

This work was supported by a Freedom of Movement grant through the Department of Orthopedics and Rehabilitation at the University of Wisconsin-Madison and a Piloting Research Innovation and Market Exploration grant through Discovery to Product at the University of Wisconsin-Madison.

References

[1] Fujie, H., Livesay, G. A., Woo, S. L., Kashiwaguchi, S., and Blomstrom, G., 1995, "The use of a universal force-moment sensor to determine in-situ forces in ligaments: a new methodology," J Biomech Eng, 117(1), pp. 1-7.

[2] Imhauser, C. W., Kent, R. N., 3rd, Boorman-Padgett, J., Thein, R., Wickiewicz, T. L., and Pearle, A. D., 2017, "New parameters describing how knee ligaments carry force in situ predict interspecimen variations in laxity during simulated clinical exams," J Biomech, 64, pp. 212-218.

[3] Gillespie, K. A., and Dickey, J. P., 2004, "Biomechanical role of lumbar spine ligaments in flexion and extension: determination using a parallel linkage robot and a porcine model," Spine (Phila Pa 1976), 29(11), pp. 1208-1216.

[4] Debski, R. E., Wong, E. K., Woo, S. L., Sakane, M., Fu, F. H., and Warner, J. J., 1999, "In situ force distribution in the glenohumeral joint capsule during anterior-posterior loading," J Orthop Res, 17(5), pp. 769-776.

[5] Debski, R. E., Parsons, I. M. t., Woo, S. L., and Fu, F. H., 2001, "Effect of capsular injury on acromioclavicular joint mechanics," J Bone Joint Surg Am, 83(9), pp. 1344-1351.

[6] Battaglia, M. J., 2nd, Lenhoff, M. W., Ehteshami, J. R., Lyman, S., Provencher, M. T., Wickiewicz, T. L., and Warren, R. F., 2009, "Medial collateral ligament injuries and subsequent load on the anterior cruciate ligament: a biomechanical evaluation in a cadaveric model," Am J Sports Med, 37(2), pp. 305-311.

[7] Cone, S. G., Lambeth, E. P., Ru, H., Fordham, L. A., Piedrahita, J. A., Spang, J. T., and Fisher, M. B., 2019, "Biomechanical Function and Size of the Anteromedial and Posterolateral Bundles of the ACL Change Differently with Skeletal Growth in the Pig Model," Clinical Orthopaedics and Related Research®, 477(9), pp. 2161-2174.

[8] Okada, Y., Teramoto, A., Takagi, T., Yamakawa, S., Sakakibara, Y., Shoji, H., Watanabe, K., Fujimiya, M., Fujie, H., and Yamashita, T., 2018, "ACL Function in Bicruciate-Retaining Total Knee Arthroplasty," J Bone Joint Surg Am, 100(17), p. e114.

[9] Sakakibara, Y., Teramoto, A., Takagi, T., Yamakawa, S., Shoji, H., Okada, Y., Kobayashi, T., Kamiya, T., Fujimiya, M., Fujie, H., Watanabe, K., and Yamashita, T., 2020, "Effect of Initial Graft Tension During Anterior Talofibular Ligament Reconstruction on Ankle Kinematics, Laxity, and In Situ Forces of the Reconstructed Graft," Am J Sports Med, 48(4), pp. 916-922.

[10] Noble, L. D., Jr., Colbrunn, R. W., Lee, D. G., van den Bogert, A. J., and Davis, B. L., 2010, "Design and validation of a general purpose robotic testing system for musculoskeletal applications," J Biomech Eng, 132(2), p. 025001.

[11] Rosvold, J. M., Darcy, S. P., Peterson, R. C., Achari, Y., Corr, D. T., Marchuk, L. L., Frank, C. B., Shrive, N. G., Rosvold, J. M., Darcy, S. P., Peterson, R. C., Achari, Y., Corr, D. T., Marchuk, L. L., Frank, C. B., and Shrive, N. G., 2011, "Technical issues in using robots to reproduce joint specific gait," J Biomech Eng, 133(5), p. 054501.

[12] Gillespie, C. M., Arant, L. R., Roth, J. D., and Colbrunn, R. W., 2024, "Sensor Fusion Algorithm to Improve Accuracy of Robotic Superposition Testing using 6-DOF Position Sensors," bioRxiv, p. 2024.2012.2016.627751.

[13] Gillespie, C., 2024, "Sensor Fusion Algorithm to Improve Accuracy of Robotic Superposition Testing Using a 6-DOF Position Sensor," Summer Biomechanics, Bioengineering, and Biotransport Conference Lake Geneva, WI.

[14] Markolf, K. L., Gorek, J. F., Kabo, J. M., and Shapiro, M. S., 1990, "Direct measurement of resultant forces in the anterior cruciate ligament. An in vitro study performed with a new experimental technique," J Bone Joint Surg Am, 72(4), pp. 557-567.

[15] Wascher, D. C., Markolf, K. L., Shapiro, M. S., and Finerman, G. A., 1993, "Direct in vitro measurement of forces in the cruciate ligaments. Part I: The effect of multiplane loading in the intact knee," J Bone Joint Surg Am, 75(3), pp. 377-386.

[16] Grood, E. S., and Suntay, W. J., 1983, "A joint coordinate system for the clinical description of three-dimensional motions: application to the knee," J Biomech Eng, 105(2), pp. 136-144.

[17] Hull, M. L., 2020, "Coordinate system requirements to determine motions of the tibiofemoral joint free from kinematic crosstalk errors," J Biomech, 109, p. 109928.

[18] Nagle, T. F., Erdemir, A., and Colbrunn, R. W., 2021, "A generalized framework for determination of functional musculoskeletal joint coordinate systems," J Biomech, 127, p. 110664.

[19] International, A., 2020, "Standard practice for use of the terms precision and bias in ASTM test methods," West Conshohocken, PA, USA.

[20] Gillespie, C. M., Haas, N. J., Nagle, T. F., and Colbrunn, R. W., 2024, "ANALYSIS AND IMPLICATIONS OF COMPLIANCE IN JOINT BIOMECHANICS SUPERPOSITION TESTING," bioRxiv, p. 2024.2012.2010.627572.

[21] Haas, N. J., Bonner, T. F., Gillespie, C. M., and Colbrunn, R. W., 2017, "Analysis of Uncertainty in Superposition Testing: Implications for Robotically Controlled Knee Joint Testing," Summer Biomechanics, Bioengineering and Biotransport ConferenceTucson, AZ.

[22] Amis, A. A., 1989, "Anterior cruciate ligament replacement. Knee stability and the effects of implants," J Bone Joint Surg Br, 71(5), pp. 819-824.

[23] Fujie, H., Sekito, T., and Orita, A., 2004, "A novel robotic system for joint biomechanical tests: application to the human knee joint," J Biomech Eng, 126(1), pp. 54-61.

[24] Darcy, S. P., Gil, J. E., Woo, S. L., and Debski, R. E., 2009, "The importance of position and path repeatability on force at the knee during six-DOF joint motion," Med Eng Phys, 31(5), pp. 553-557.

[25] Goldsmith, M. T., Smith, S. D., Jansson, K. S., LaPrade, R. F., and Wijdicks, C. A., 2014, "Characterization of robotic system passive path repeatability during specimen removal and reinstallation for in vitro knee joint testing," Med Eng Phys, 36(10), pp. 1331-1337.

[26] Howard, R. A., Rosvold, J. M., Darcy, S. P., Corr, D. T., Shrive, N. G., Tapper, J. E., Ronsky, J. L., Beveridge, J. E., Marchuk, L. L., and Frank, C. B., 2007, "Reproduction of in vivo motion using a parallel robot," J Biomech Eng, 129(5), pp. 743-749.

[27] Crameri, F., Shephard, G. E., and Heron, P. J., 2020, "The misuse of colour in science communication," Nat Commun, 11(1), p. 5444.

Figures

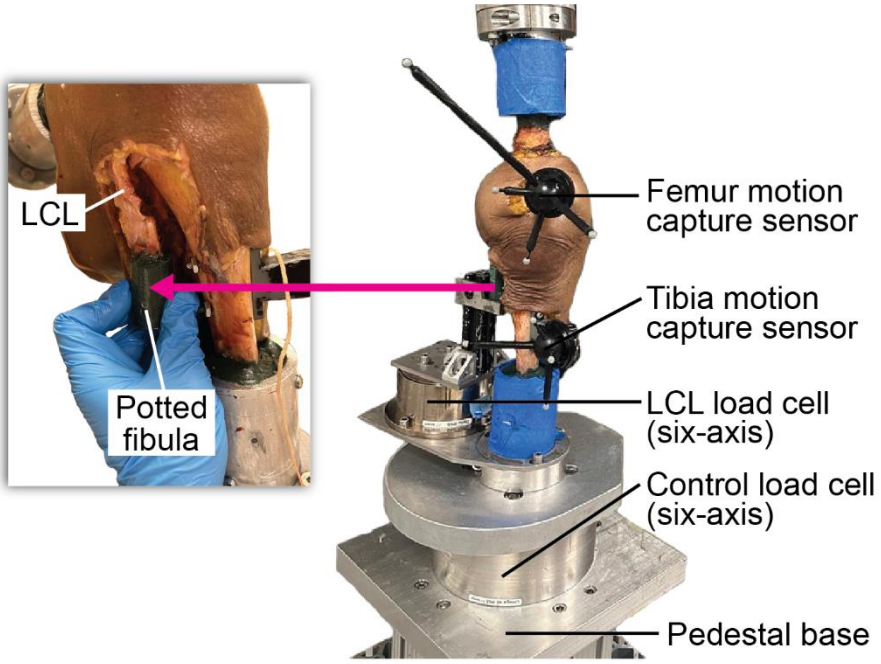

Figure 1: To directly measure gold-standard lateral collateral ligament (LCL) tension, we embedded the inferior end of the proximal fibula and an aluminum core in Bondo for rigid fixation to a six-axis load cell. We ensured that the load cell was only measuring LCL tension by resecting all other soft tissues attached to the fibular head and resecting the articular surfaces of the proximal tibiofibular joint.

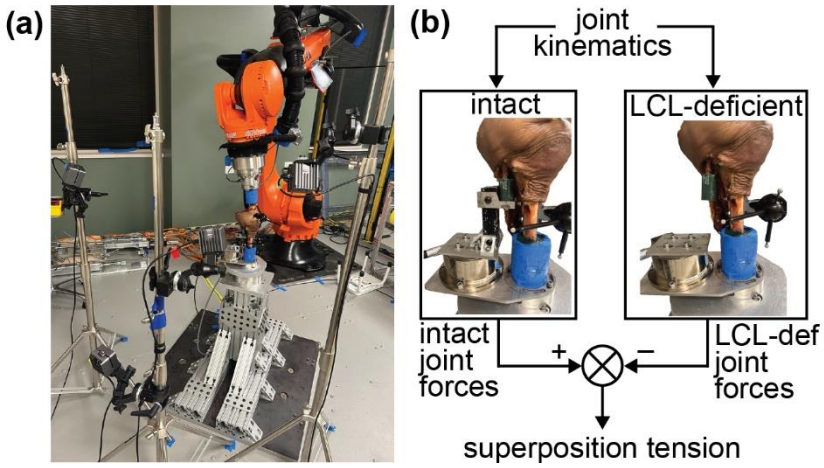

Figure 2: (a) We prescribed varus and external rotation loading using a six-degree-of-freedom robotic testing system. We used optical motion capture to define an initial joint coordinate system and to measure joint kinematics. **(b)** We computed superposition tension using the vector difference in joint forces between the intact and lateral collateral ligament-deficient (LCL-def) joints [1].

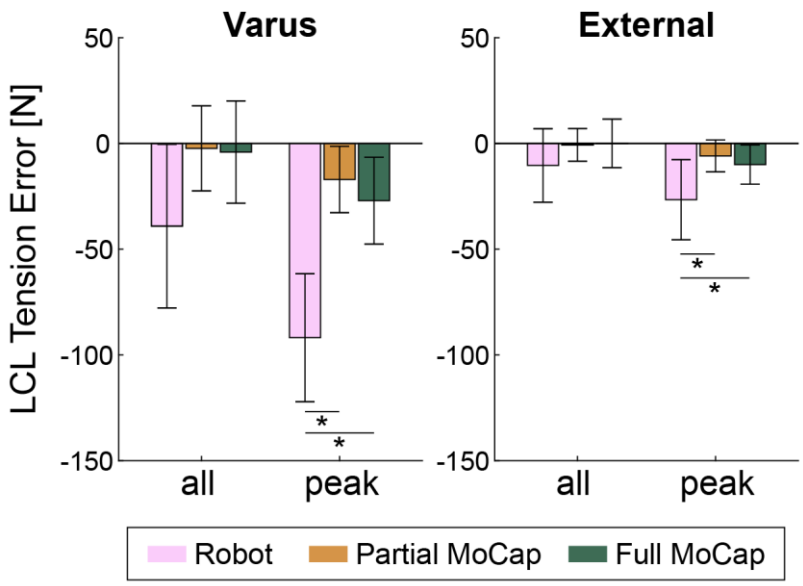

Figure 3: The bars and error bars represent the bias errors and precision errors, respectively, in superposition-computed LCL tensions for the robot, partial motion capture (MoCap) and full MoCap control methods. The "all" data includes errors for all timepoints in the load-unload ramp trajectory, and the "peak" data includes only errors at the peak LCL tension. *$p<0.05$ from linear mixed models with post-hoc Tukey tests. In all results figures, we used colors accessible to those with color-vision deficiencies [27].

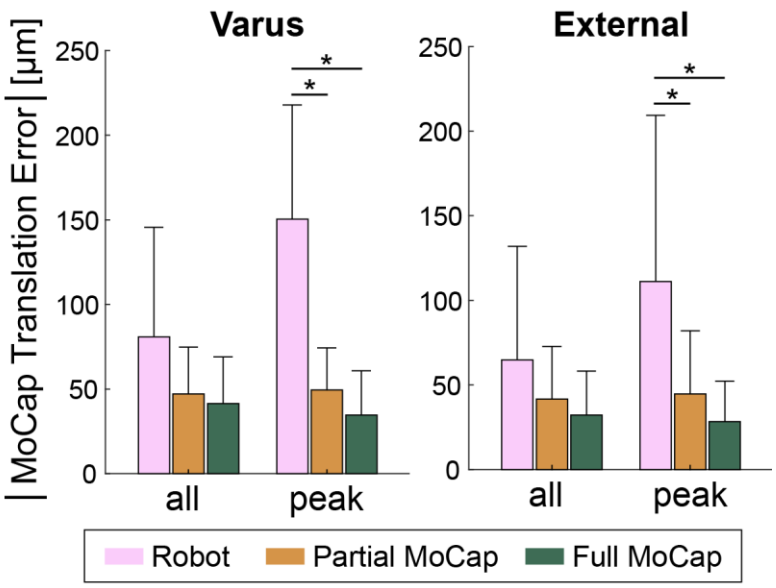

Figure 4: The bars and error bars represent the bias and precision, respectively, of the magnitude of the errors in motion capture translations between the intact and LCL-deficient states for the robot, partial motion capture (MoCap) and full MoCap control methods. The "all" data includes errors for all timepoints in the load-unload ramp trajectory, and the "peak" data includes only errors at the peak LCL tension. *$p<0.05$ from linear mixed models with post-hoc Tukey tests

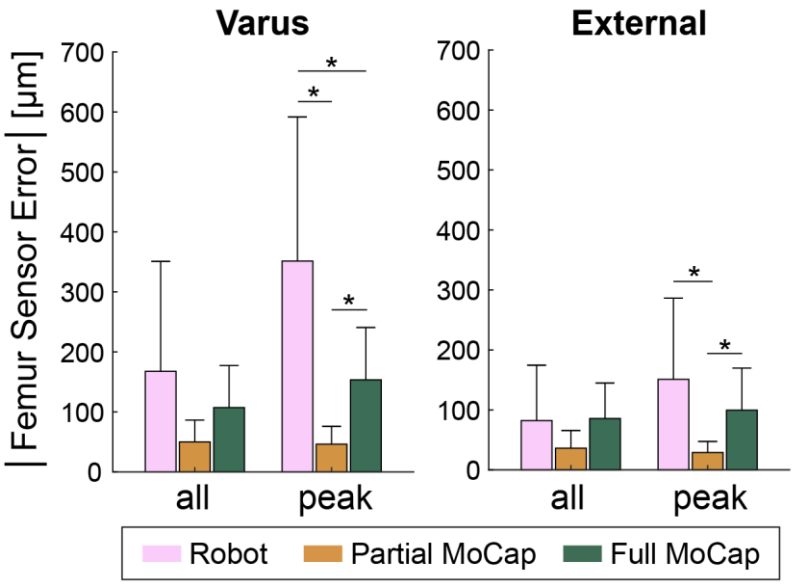

Figure 5: The bars and error bars represent the bias and precision, respectively, of the magnitude of the errors in the position of the femur sensor between the intact and LCL-deficient states for the robot, partial motion capture (MoCap) and full MoCap control methods. The "all" data includes errors for all timepoints in the load-unload ramp trajectory, and the "peak" data includes only errors at the peak LCL tension. *$p<0.05$ from linear mixed models with post-hoc Tukey tests

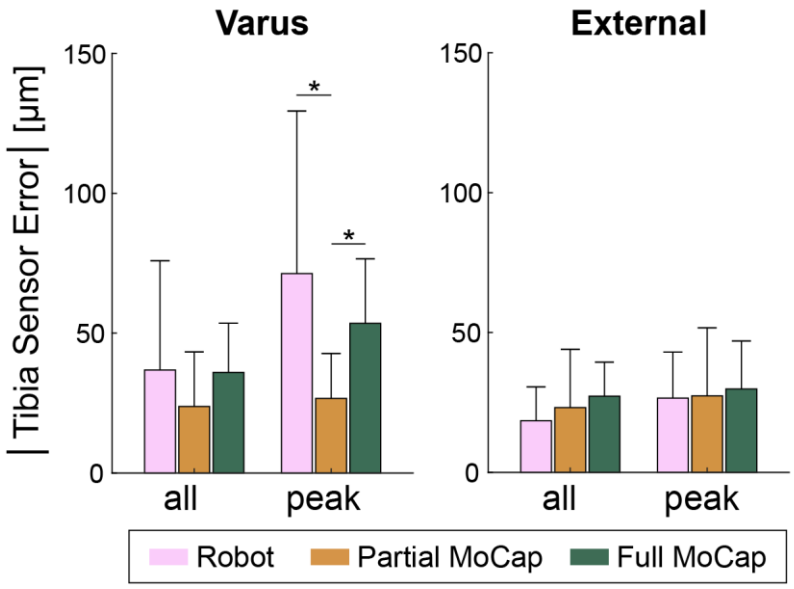

Figure 6: The bars and error bars represent the bias and precision, respectively, of the magnitude of the errors in the position of the tibia sensor between the intact and LCL-deficient states for the robot, partial motion capture (MoCap) and full MoCap control methods. The "all" data includes errors for all timepoints in the load-unload ramp trajectory, and the "peak" data includes only errors at the peak LCL tension. *$p<0.05$ from linear mixed models with post-hoc Tukey tests

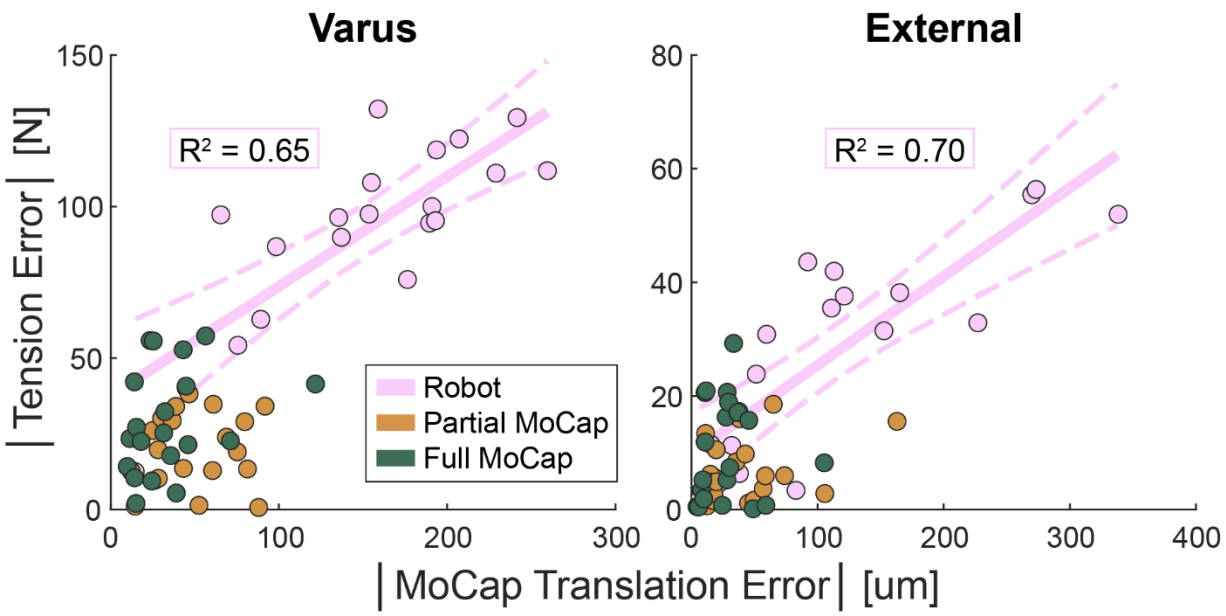

Figure 7: There were significant, positive relationships between the magnitude of the motion capture (MoCap) translation errors and the magnitude of the superposition-computed tension errors at peak tension for the robot control method, but not the partial or full motion capture control methods.

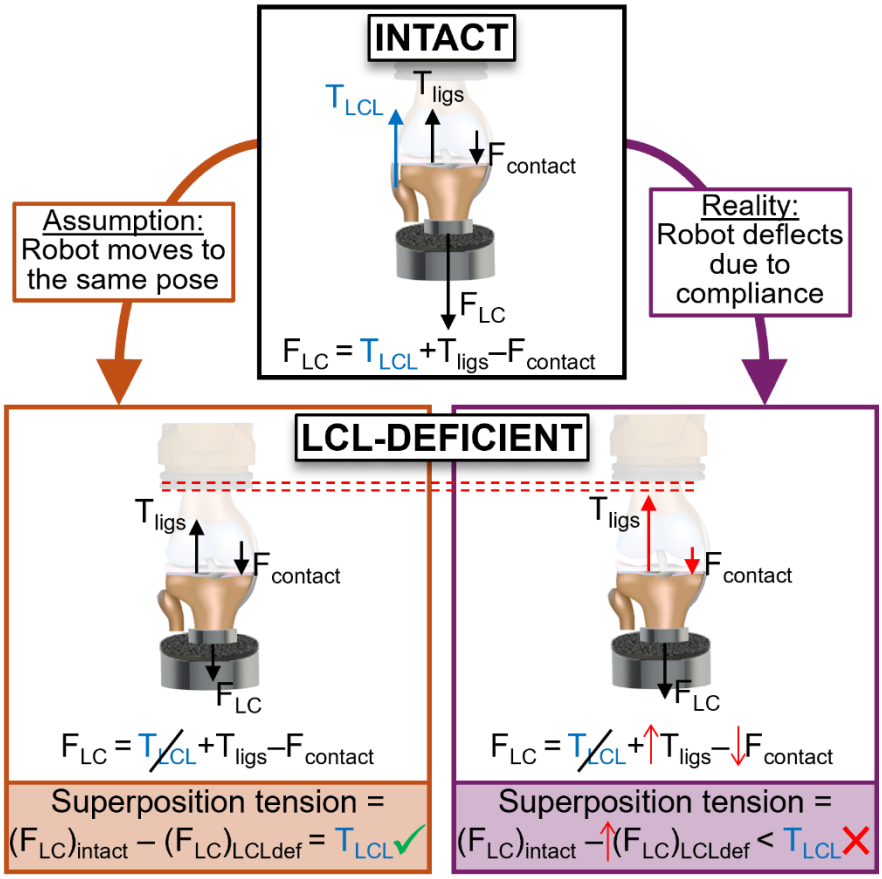

Figure 8: This simplified two-dimensional analysis demonstrates that if system compliance is negligible, then the difference in control load cell forces between the intact and ligament-deficient joints can be used to compute ligament tension. However, every test system has some compliance, and thus, the difference in control load cell forces underestimates the true ligament tension. Abbreviations: T_{LCL} = lateral collateral ligament tension, T_{ligs} = tension in secondary restraints, $F_{contact}$ = contact force, F_{LC} = force measured by the control load cell

Tables

Table 1: We measured joint kinematics using three different methods for tracking the femur and the tibia.

Kinematic measurement	Femur tracking	Tibia tracking
Robot kinematics	Robot end effector	Assumed fixed
Full motion capture kinematics	Motion capture sensor	Motion capture sensor
Partial motion capture kinematics	Motion capture sensor	Assumed fixed

Supplements

S.1 Load cell specifications

The specifications of each of the six-axis load cells are found in **Table S1**. The LCL load cell was the ATI Delta IP65 load cell with SI-660-60 calibration. The robot control load cell was the ATI Omega160 IP65 with SI-1000-120 calibration.

Table S1: Manufacturer-reported sensing ranges and resolutions of the six-axis load cells used in this study.

	Sensing ranges				Resolutions			
	Fx, Fy [N]	Fz [N]	Tx, Ty [Nm]	Tz [Nm]	Fx, Fy [N]	Fz [N]	Tx, Ty [Nm]	Tz [Nm]
LCL load cell	660	1980	60	60	1/8	1/4	10/1333	10/1333
Control load cell	1000	2500	120	120	1/4	1/4	1/40	1/80

S.2 Stiffness of LCL load cell fixture

We measured the stiffness of the stainless-steel plate used to attach the LCL load cell to the pedestal base to confirm that this fixture was not deflecting under the applied LCL tensions. First, we attached the LCL load cell fixture to the pedestal base as it was attached to measure the LCL tension in the cadaver knees (**Fig. S1**). Next, we attached one end of a rope to the location of the potted fibula attachment on the LCL load cell fixture. We attached the other end of the rope to the robot end effector, which was positioned directly above the potted fibula attachment to replicate the line of action of the LCL. We also attached a motion capture sensor with four 0.25-inch diameter markers to the stainless-steel plate used to connect the LCL load cell to the pedestal base. We used the robot to prescribe tensile loads in approximately 25 N increments to the fixture up to 230 N. We chose 230 N as the peak applied load because this was the maximum LCL

tension measured during this experiment. At each load level, we measured the resultant force using the LCL load cell and the resultant displacement of the stainless-steel plate using the motion capture sensor. The motion capture sensor was tracked using our four calibrated optical motion capture cameras (Optitrack Prime 13×; NaturalPoint Inc.). We repeated this process of loading the fixture and measuring the resultant forces and motion capture sensor displacements for three repeated trials.

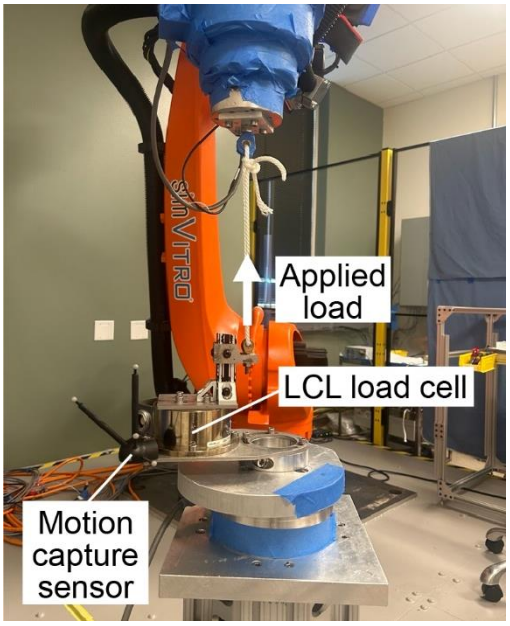

Figure S1: We measured the stiffness of the stainless-steel plate used to connect the lateral collateral ligament (LCL) load cell to the pedestal base by applying loads to the LCL load cell fixture and measuring the resultant displacement of the plate using an optical motion capture sensor.

For each trial, we computed the stiffness of the LCL load cell plate as the slope of the resultant force vs. resultant motion capture sensor displacement relationship during loading (all trials $R^2 > 0.99$). We determined the stiffness of the LCL load cell plate to be 2196 ± 32 N/mm.

S.3 Measurement errors of optical motion capture system

To quantify the errors of our motion capture system, we measured the errors in the tracked displacement of a motion capture marker. We quantified these errors with four calibrated optical motion capture cameras (Optitrack Prime 13×; NaturalPoint Inc.) positioned to replicate their configuration during the cadaveric experiments (**§2.2**). To prescribe displacements, we used a linear stage fixed to the pedestal base (**Fig. S2**). To measure gold-standard displacements, we positioned a dial indicator (resolution of 1 μm) in contact with the linear stage parallel to its translation axis. We attached a 0.25-inch motion capture marker to the tip of the dial indicator. Starting with the translation axis of the linear stage approximately perpendicular to the camera plane, we translated the marker using the linear stage in 2 mm increments until 24 mm of displacement was reached. At each increment, we recorded the marker displacement as measured by our motion capture system and by the dial indicator. We then rotated the linear stage in 10° increments about a vertical axis up to a maximum of 90°. At each rotation, we reset the linear stage to 0 mm of translation and repeated the measurements of marker displacements at every 2 mm of stage translation. At 90° rotation, the translation axis of the linear stage was approximately parallel with the plane of the cameras.

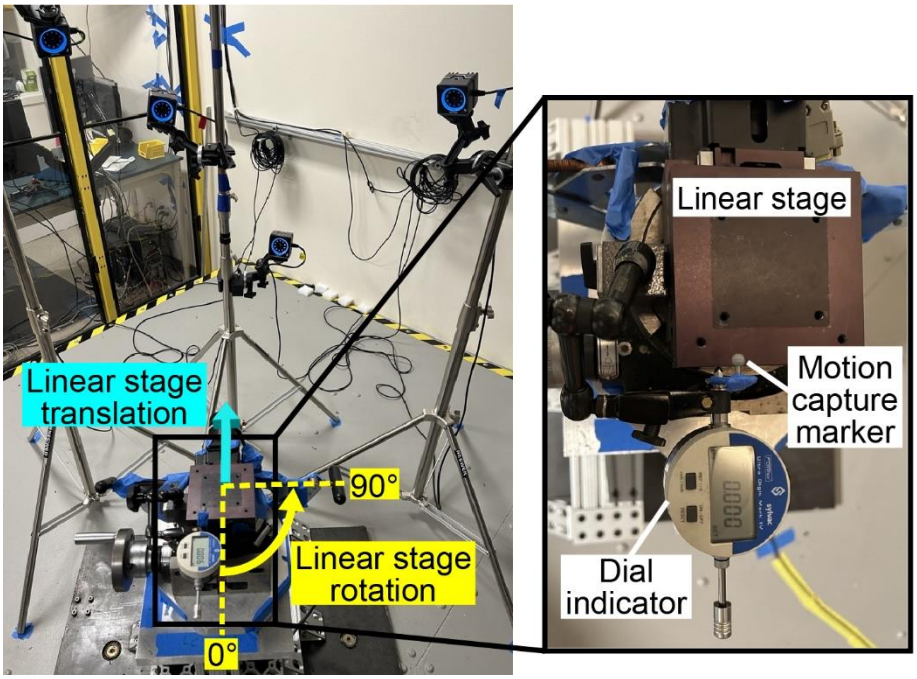

Figure S2: We computed the errors in marker displacement between those measured by our motion capture system and those measured by a dial indicator for varying translations and rotations of a linear stage.

We computed the errors in the motion capture marker displacements as the difference between the displacements measured by the motion capture system and those measured by the dial indicator. We pooled the errors across all of the stage translations and orientations and computed the bias (mean) and precision (standard deviation) errors to be 19 ± 56 μm. We computed the root mean square error to be 59 μm.

S.4 Stiffness of robotic testing system

We measured the stiffness of our robotic testing system (KR300-R2700; KUKA Robotics) by prescribing loads and measuring the resulting displacement of the end effector (**Fig. S3**). During all testing, the robot was posed in its home position with each of its drives turned on. The home position is near the typical pose of the robot with a knee in full extension. We prescribed loads to the robot by manually pulling on the end effector

using a rope in each of the six directions with respect to the robot base coordinate system (i.e., +X, -X, +Y, -Y, +Z, -Z). We reached a peak load of at least 800 N in each of these directions except for +X. We only reached a peak load of 645 N in +X to minimize the risk of bumping the optical motion capture cameras during loading. We measured the prescribed loads using a six-axis load cell mounted to the robot end effector, and we measured the robot displacement by attaching a motion capture sensor with four 0.25-inch diameter markers to the robot end effector. The motion capture sensor was tracked using our four calibrated optical motion capture cameras (Optitrack Prime 13×; NaturalPoint Inc.).

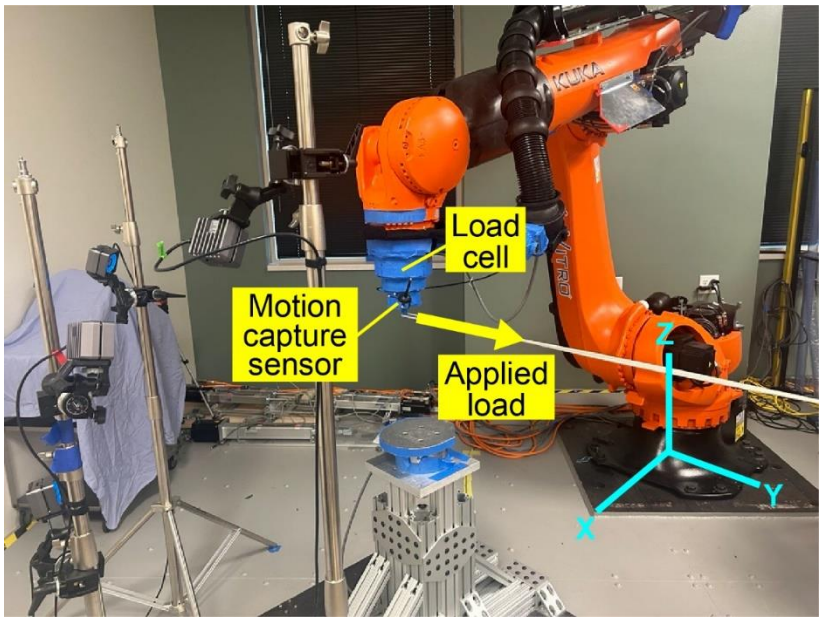

Figure S3: We measured the stiffness of the robot in its home position by manually applying loads to the end effector (e.g., in +Y direction, as shown in this figure) and measuring the resulting displacement of the end effector.

To compute the stiffness in each direction, first, we low-pass filtered the motion capture sensor and load cell data using a 2 Hz cut-off frequency. Then, we computed the resultant motion capture sensor displacements and load cell forces. Finally, we extracted

the robot stiffness as the slope of the resultant force vs. resultant motion capture sensor displacement relationship during loading (range of R^2 = 0.95 to 0.99). The stiffness of our robot was greatest in the X direction and smallest in the Y direction (**Table S2**). For context, the Z direction is most closely aligned with the compression-distraction direction of the knee joint during robotic testing. These stiffnesses are comparable to those measured in serial Kuka robots of similar size [20, 21].

Table S2: Robot stiffnesses in each direction with respect to the robot base coordinate system.

Direction	Stiffness (N/mm)
-X	1107
+X	1338
-Y	551
+Y	562
-Z	804
+Z	597

S.5 Preconditioning

Before superposition testing, we preconditioned the soft tissues in each knee. We prescribed 10 cycles of each of the varus and external rotation loading trajectories at each flexion angle. We measured the peak lateral collateral ligament (LCL) tension during each cycle using the LCL load cell and computed the change in the peak LCL tension between consecutive cycles. By the tenth cycle, the change in peak tension was less than 2 N for all loading trajectories in all specimens except one (**Fig. S4**). The maximum change in peak tension in the tenth cycle was only 4 N during varus loading at 60° flexion, which is a 4% change. Thus, we deemed the preconditioning satisfactory for this study.

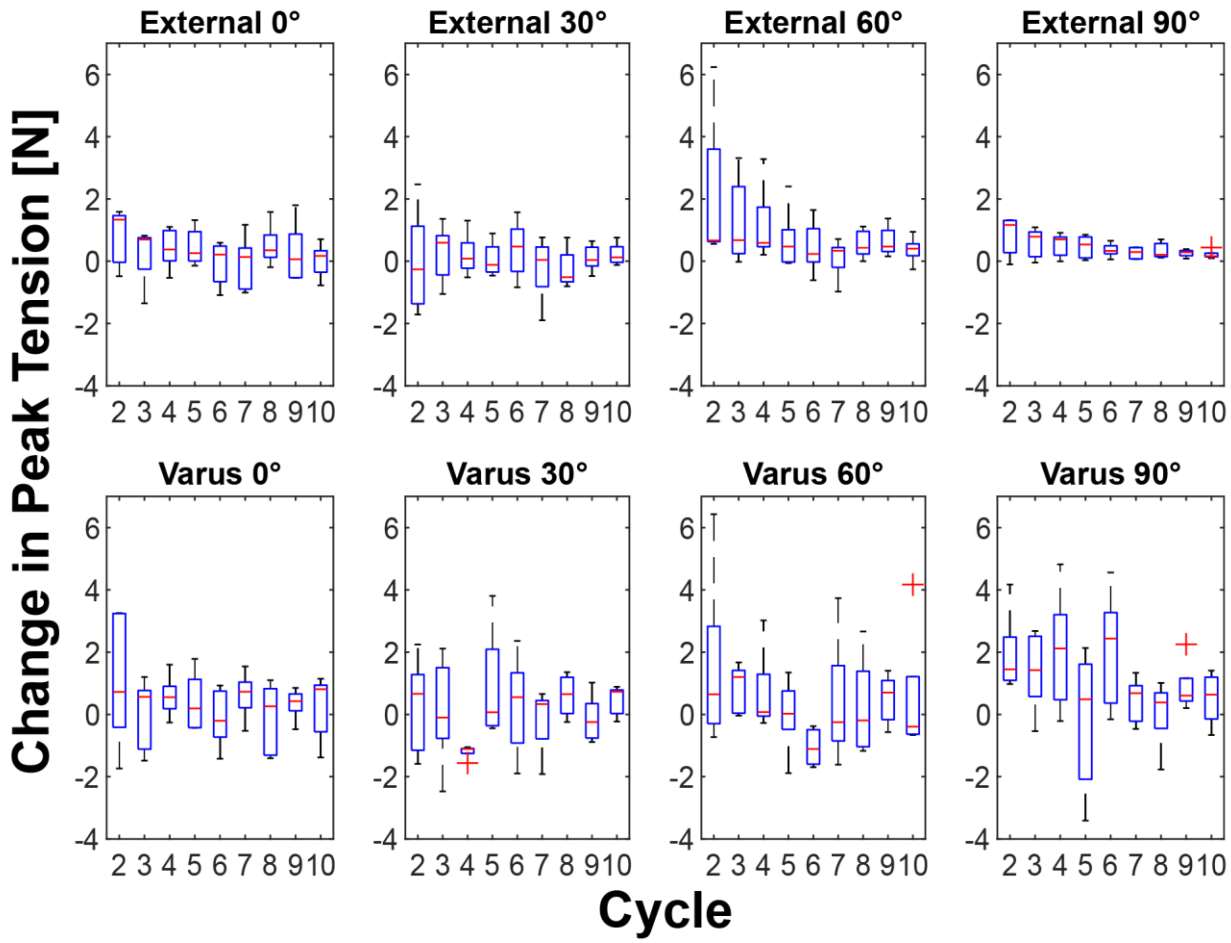

Figure S4: Change in the peak lateral collateral ligament tension between consecutive cycles during preconditioning. The box plots depict summary statistics for data pooled across the five specimens.

S.6 Kinematic tracking errors

To quantify the performance of the kinematic controller, we computed the errors in kinematic tracking as the difference between the measured and desired kinematics in each degree of freedom for each trial. The kinematic variable used in the computation was the variable being controlled (i.e., kinematic error for partial motion capture control was the error between the measured and desired partial motion capture kinematics). We pooled the errors across specimens, flexion angles, and ligament conditions, and

computed the root mean square error for each degree of freedom (**Table S3**). The kinematic tracking errors were all under 100 μm or 100 μ°, which are over an order of magnitude less than the excursions of the knees during testing. Therefore, we considered the performance of the kinematic controller to be adequate.

Table S3: Root mean square errors in kinematic tracking between the desired and measured kinematics. Abbreviations: MoCap = motion capture

	Control method	Medial [μm]	Posterior [μm]	Superior [μm]	Flexion [μ°]	Valgus [μ°]	Internal rotation [μ°]
Varus	Robot	20	21	40	2	22	24
	Partial MoCap	33	30	36	18	22	25
	Full MoCap	31	29	37	21	25	25
External	Robot	20	75	36	2	6	76
	Partial MoCap	33	78	35	18	9	78
	Full MoCap	32	75	35	16	10	78